2012

Conversion Reactions in Surface-Functionalized Mesoporous Materials: Effect of Restricted Transport and Catalytic Site Distribution

Jing Wang
Iowa State University, jingw@iastate.edu

David Ackerman
Iowa State University, ackerman@iastate.edu

Kapil Kandel
Iowa State University

Igor I. Slowing
Iowa State University, islowing@iastate.edu

Marek Pruski
Iowa State University, mpruski@iastate.edu

Conversion Reactions in Surface-Functionalized Mesoporous Materials: Effect of Restricted Transport and Catalytic Site Distribution

Abstract
We analyze the interplay between anomalous transport and conversion reaction kinetics in mesoporous materials functionalized with catalytic groups. Of primary interest is functionalized mesoporous silica containing an array of linear pores with diameters tunable from 2-10 nm, although functionalization can produce smaller effective diameters, d. For d < 2 nm, transport and specifically passing of reactant and product species within the pores can be strongly inhibited (single-file diffusion). The distribution of catalytic groups can also vary depending on the synthesis approach. We apply statistical mechanical modeling (utilizing spatially discrete stochastic lattice-gas models) to explore the dependence of reactivity on the extent of inhibition of passing of species within the pore, as well as on the distribution of catalytic sites.

Keywords
catalytic, infiltration (chemical reaction), diffusion

Disciplines
Chemistry

Comments
This article is from *MRS Proceedings* 1423 (2012): 6 pp., doi:10.1557/opl.2012.229. Posted with permission.

Authors
Jing Wang, David Ackerman, Kapil Kandel, Igor I. Slowing, Marek Pruski, and James W. Evans

Mater. Res. Soc. Symp. Proc. Vol. 1423 © 2012 Materials Research Society
DOI: 10.1557/opl.2012.229

Conversion Reactions in Surface-Functionalized Mesoporous Materials: Effect of Restricted Transport and Catalytic Site Distribution

Jing Wang[1,2], David M. Ackerman[1,3], Kapil Kandel[1,3], Igor I. Slowing[1], Marek Pruski[1,3] and James W. Evans[1,2,4]
[1]Ames Laboratory – USDOE, and Departments of [2]Mathematics, [3]Chemistry, and [4]Physics & Astronomy, Iowa State University, Ames, IA 50011, U.S.A.

ABSTRACT

We analyze the interplay between anomalous transport and conversion reaction kinetics in mesoporous materials functionalized with catalytic groups. Of primary interest is functionalized mesoporous silica containing an array of linear pores with diameters tunable from 2-10 nm, although functionalization can produce smaller effective diameters, d. For $d < 2$ nm, transport and specifically passing of reactant and product species within the pores can be strongly inhibited (single-file diffusion). The distribution of catalytic groups can also vary depending on the synthesis approach. We apply statistical mechanical modeling (utilizing spatially discrete stochastic lattice-gas models) to explore the dependence of reactivity on the extent of inhibition of passing of species within the pore, as well as on the distribution of catalytic sites.

INTRODUCTION

Functionalized mesoporous materials integrate the selectivity of homogeneous catalysts with the stability and separability of heterogeneous catalysts [1,2]. In the case of mesoporous silica, nanospheres with diameters of the order of 100 nm are synthesized via a soft-templating technique wherein a silica precursor (TEOS) aggregates around a self-assembled array of cylindrical CTAB micelles. Removal of CTAB produces mesoporous silica nanospheres (MSN) with a hexagonal arrangement of parallel linear nanopores with nominal pore diameters of around 2 nm or larger [3]. Control of surface properties is achieved by functionalization with suitable anchored groups serving as catalysts, and sometimes by additional groups modifying selectivity by acting as "gatekeepers" near the pore openings [4], or tuning activity (e.g., by strongly interacting with one of the products to alter the reaction equilibrium [5]).

Functionalization by grafting of these groups after formation of the MSN should produce a higher loading of catalytic groups near the pore openings and likely also populate the exterior surface. In contrast, co-condensation during nanosphere formation produces a more uniform distribution within the pores. For MSN, it is significant to note that functionalization can reduce the effective diameter, d, *below* 2 nm. Then, transport can be strongly inhibited. The extreme case of "no passing" of reactants and products corresponds to so-called single-file diffusion [6].

There have been extensive studies of single-file diffusion systems often motivated by studies of transport and catalytic reaction in zeolites [7]. Typically, these studies emphasize the anomalous nature of tracer- or self-diffusion, this anomaly being reflected in a sub-linear increase (vs. a conventional linear increase) with time in mean-square displacement of a specific "tagged" particle [6]. Our interest is in the interplay between this type of anomalous transport and the catalytic reaction kinetics. Such behavior is traditionally described by reaction-diffusion equations (RDE). However, characterization of chemical diffusion (rather than tracer diffusion), which provides key input to these equations, has received relatively little attention for quasi-single-file systems. Its correct description is a non-trivial statistical mechanical challenge.

Our focus in this contribution is on simple first-order catalytic conversion reactions (A→B) in systems with linear nanopores. A key factor impacting reactivity is the extent to which reactants and products A and B can pass each other. Passing of A with other A (or B with B) is not significant. Several previous analyses exist for the case of single-file diffusion [8-15] revealing that reactivity is strongly localized near the pore openings in this case of no-passing [9]. A perception exists that a simple mean-field (MF) type treatment of chemical diffusion (see below) is adequate [11]. Unfortunately, this is not true in regimes with large variations in the magnitude of rates for various processes (e.g., low reaction versus diffusion rates). This feature motivated our development of an alternative "hydrodynamic" description of chemical diffusion which effectively captures the single-file constraint [13]. However, this formulation did not incorporate finite-size or fluctuation effects, so additional refinement was necessary to achieve quantitative predictive capability [14,15]. We also note that an effective alternative for precise characterization of model behavior is Kinetic Monte Carlo (KMC) simulation.

In this paper, we apply statistical mechanical modeling (adopting spatially discrete stochastic lattice-gas models) to analyze A→B conversion reactions in linear nanopores with inhibited transport. Specifically, we explore the dependence of reactivity on the extent of inhibition of passing of species within the pore, as well as on the distribution of catalytic sites. We focus on precise characterization of model behavior (as is readily achieved, e.g., by KMC simulation) rather than on the above-mentioned development of theoretical methodology.

CATALYTIC CONVERSION REACTION IN A LINEAR NANOPORE: LG MODEL

Stochastic Lattice-Gas (LG) Reaction-Diffusion Model Prescription

In our model for A→B conversion (see Fig.1), species within a pore are localized to sites (or cells) of a 1D linear lattice traversing that pore. The cell width "a" is selected as comparable to the species size (~1 nm). To describe the surrounding fluid, we extend the 1D lattice inside the pores to a 3D lattice outside. We specify "external" reactant and product concentrations in the surrounding fluid as $\langle A_{out} \rangle$ and $\langle B_{out} \rangle$. These give the probabilities that sites or cells on the 3D lattice are occupied, where fluid cell occupation is assumed random due to efficient stirring.

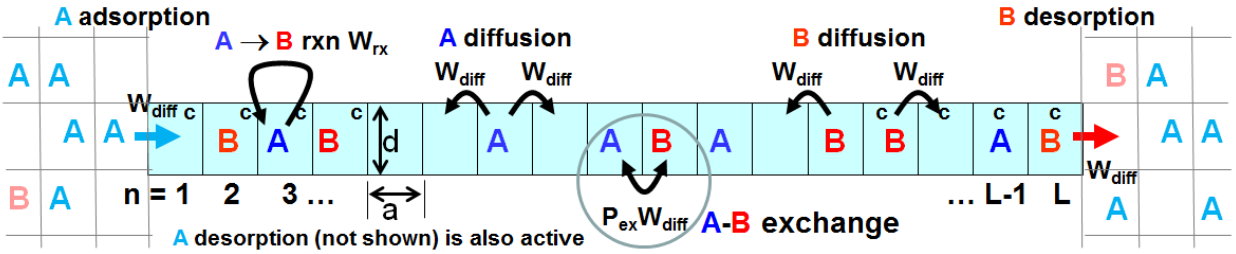

Figure 1. Schematic of the LG conversion reaction model illustrating processes within a single pore (shaded light blue), as well as coupling to the surrounding fluid. 'c' denotes catalytic sites.

The simplest prescription for diffusion within the pores is that A and B hop to adjacent empty (E) sites at rate W_{diff}. This would correspond to single-file diffusion with a strict no-passing constraint. We also allow positional exchange of adjacent A and B at rate $W_{ex} = W_{diff} P_{ex}$ to relax the strict single-file constraint, noting that exchange of adjacent particles of the same type has no effect. The passing propensity, $P_{ex} = P_{ex}(d)$, will increase with the effective pore

diameter, d (from $P_{ex} = 0$ for d below a threshold where passing is strictly excluded due to steric effects, to $P_{ex} = 1$ for large d and unhindered passing). The other mechanistic steps in the model are: **(i)** Adsorption of external species at terminal sites of the pore at rate $W^A_{ads} = W_{diff} <A_{out}>$ ($W^B_{ads} = W_{diff} <B_{out}>$) for the reactant (product), provided that these end sites are unoccupied or empty (E); **(ii)** Desorption of both the reactant, A, and product, B, from terminal sites of the pore at rate W_{diff} provided that the fluid site just outside the pore is unoccupied (E_{out}). Since fluid sites are occupied with probability $<X_{out}> = <A_{out}> + <B_{out}> = 1 - <E_{out}>$, desorption of A and B occurs with effective rate $W_{des} = W_{diff} <E_{out}>$; **(iii)** Conversion $A \rightarrow B$ at catalytic (c) sites within the pore at rate W_{rx}; c-sites may occupy all or just some sites within the pore. See Fig.1.

For our rates, the dynamics for particles X=A+B is a non-reactive diffusion process. In the steady state, sites are randomly occupied by particles, X, with probability $X_{eq} = <X_{out}>$ [12].

Master Equations and Reaction-Diffusion Equations (RDE)

Sites within the pore(s) are labeled by n=1, 2,…, L (for pore length L), so terminal sites are n=1 and n=L. An exact description of our discrete reaction-diffusion model is provided by the master equations for the evolution of probabilities of various configurations within the pore. Often these are written in hierarchical form [8,11,12-14]. Here, we use $<C_n>$ to denote the probability or ensemble averaged concentration for species C = A or B at site n, $<C_nE_{n+1}>$ for the probability that C is at site n and for site n+1 to be empty (E), etc. Then, the lowest-order equations in the hierarchy describe the evolution of single-site occupancies.

For $A \rightarrow B$ conversion in the case where *all sites are catalytic*, one has that [12-14]

$$d/dt <A_n> = -W_{rx}<A_n> - \nabla J_A^{n>n+1},\ d/dt <B_n> = +W_{rx}<A_n> - \nabla J_B^{n>n+1},\ \text{for } 1<n<L. \quad (1)$$

with separate equations for terminal sites reflecting adsorption-desorption boundary conditions (BC's), e.g., $d/dt <A_1> = W^A_{ads} <E_1> - W_{des} <A_1> - W_{rx} <A_1> - J_A^{1>2}$. In (1), we have defined the discrete derivative, $\nabla K_n = K_n - K_{n-1}$. The *net* flux, $J_A^{n>n+1}$, of A from site n to n+1 is given by

$$J_A^{n>n+1} = W_{diff} [<A_nE_{n+1}> - <E_nA_{n+1}>] + W_{ex} [<A_nB_{n+1}> - <B_nA_{n+1}>]. \quad (2)$$

The expression for the net flux, $J_B^{n>n+1}$, of B is analogous. In the special case $P_{ex} = 1$ where $W_{ex} = W_{diff}$, transport of A including passing of B is completely unhindered (the opposite of single-file diffusion). Then, (2) reduces exactly to $J_A^{n>n+1} = W_{diff} [<A_n> - <A_{n+1}>] = -W_{diff} \nabla <A_n>$ (cf. Ref. [16]). If some sites are not catalytic, then the reaction terms are absent for such sites. The total rate of production of B is given by $R^B_{tot} = W_{rx} \sum_{n=c} <A_n>$, summing over all catalytic sites.

Equations (1) couple to various pair probabilities in (2). Pair probability evolution is coupled to triples, etc., producing a hierarchy. Pair, etc., probabilities are not simply related to single-site probabilities due to spatial correlations. A simple MF factorization approximation, $<C_nE_{n+1}> \approx <C_n><E_{n+1}>$, etc., produces a closed set of discrete reaction-diffusion equations (dRDE) for single-site concentrations. A higher-level pair approximation retains pair quantities, but factorizes triplets, e.g., $<C_nM_{n+1}N_{n+2}> \approx <C_nM_{n+1}><M_{n+1}N_{n+2}>/<M_{n+1}>$, with C, M, N = A, B, or E. This generates a closed set of equations for single-site and pair quantities [8,11,12-14].

For smoothly varying concentrations within the pore, it is natural to consider a coarse-grained description where species concentrations per unit length are $K(x=na) \approx a^{-1} <K_n>$, leaving the t-dependence implicit. Below, we set a=1. The continuum or hydrodynamic RDE (hRDE) for our $A \rightarrow B$ conversion reaction model with all sites catalytic then have the form [12-14]

$$\partial/\partial t\, A(x) = -W_{rx}(A)\, A(x) - \partial/\partial x\, J_A, \quad \partial/\partial t\, B(x) = +W_{rx}(A)\, A(x) - \partial/\partial x\, J_B. \qquad (3)$$

If only portions of the pore are catalytic, reaction terms appear just for those locations. BC's for (3) at the pore ends reflect the adsorption-desorption dynamics [13]. Description of the diffusion fluxes, J_C, for C = A and B is non-trivial. In the steady-state with uniform total concentration, X_{eq}, we write $J_C = -D_{tr}(X_{eq})\, \partial/\partial x\, C(x)$ where D_{tr} is a tracer diffusion coefficient [13-15]. The MF treatment sets $D_{tr} = (1 - X_{eq})W_{diff}$ [12,13] overestimating fluxes. In a classic hydrodynamic treatment, one has $D_{tr} \sim W_{diff}/L \to 0$, as $L \to \infty$ [14], underestimating fluxes. Precise fluxes follow from a generalized hydrodynamic treatment where D_{tr} is enhanced near pore openings [15].

CATALYTIC REACTION KINETICS: LG MODEL PREDICTIONS

Pore completely functionalized with catalytic sites

For the case where all sites within the pore are catalytic, Fig.2a compares steady-state concentration profiles for $\langle A_n \rangle$ and $\langle B_n \rangle$ versus n for single-file diffusion ($P_{ex} = 0$), hindered passing of A and B with $P_{ex} = ¼$, and completely unhindered passing (standard diffusion) where $P_{ex} = 1$. Other model parameters are specified in the caption (reflecting the initial stages of reaction with no significant buildup $\langle B_{out} \rangle$). The most dramatic feature is the strongly enhanced penetration of reactant into the pore with increasing propensity, P_{ex}, of passing of A and B. Correspondingly, the reaction rate, R^B_{tot}, increases strongly increasing P_{ex} as shown in Fig.2c.

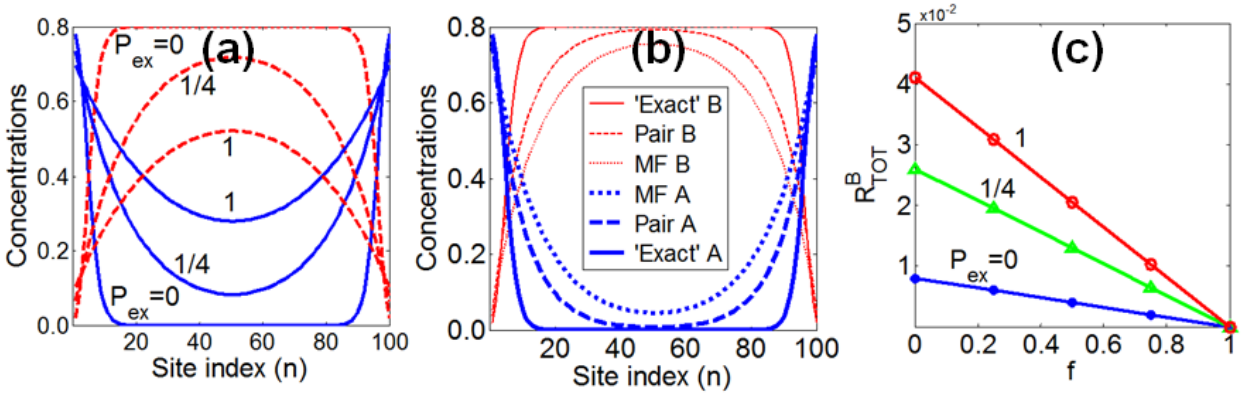

Figure 2. Steady-state concentration profiles for model parameters L=100, $W_{rx} = 0.001$, $W_{diff} = 1$, $\langle A_{out} \rangle = 0.8$, and $\langle B_{out} \rangle = 0$: **(a)** dependence on the propensity for passing of reactants and products ($P_{ex} = 0, ¼, 1$); A (B) is blue, solid (red, dashed); **(b)** comparison of exact profiles for $P_{ex} = 0$ (single-file diffusion) with those predicted by MF and pair approximations; A (blue) is minimum and B (red) is maximum at the pore center. **(c)** Reaction rate, $R^B_{tot}(f)$, versus fraction of conversion of reactant to product, $f = (X_{eq} - \langle A_{out} \rangle)/X_{eq} = \langle B_{out} \rangle / X_{eq}$, for $P_{ex} = 0, ¼$, and 1.

Given our remarks on the short-comings of MF-type treatments of chemical diffusion, it is appropriate to show the extent of this failure for the above example for single-file diffusion. (The MF treatment becomes more accurate with increasing P_{ex}, and is actually exact for $P_{ex} = 1$.) Fig.2b compares exact behavior with that obtained from the standard MF approximation and also the pair approximation. The MF approximation greatly overestimates diffusion fluxes in the steady-state, and thus also the extent of penetration of reactant into the pore and the reactivity.

The pair approximation, which at least approximately accounts for the effect of spatial correlations, shows significant improvement over MF predictions, but is still far from precise.

Next, we characterize behavior during the "extended reaction" for the above parameter choice as a significant fraction, f, of reactant outside the pore becomes converted to product. During the extended reaction, $\langle A_{out} \rangle$ decreases and $\langle B_{out} \rangle$ increases while $\langle X_{out} \rangle = \langle A_{out} \rangle + \langle B_{out} \rangle = 0.8 = X_{eq}$ remains constant. Thus, one has $f = (X_{eq} - \langle A_{out} \rangle)/X_{eq} = \langle B_{out} \rangle / X_{eq}$. Since the volume and thus the amount of reactant and product outside the pores far exceeds that inside, this induces a separation of time scales in the system. The characteristic time for change of $\langle A_{out} \rangle$ far exceeds that for relaxation to steady-state of the concentration distribution inside the pores. Thus, one can perform a sequence of simulations for different values of conversion, f, to determine the associated reaction rate, R^B_{tot} , then interpolate these results to obtain the variation of R^B_{tot} during the extended reaction. This yields the complete kinetics for conversion of A to B.

The results of this analysis shown in Fig.2c reveal that the reaction rate decreases linearly as a function of f. This reflects the linearity of the governing master equations or RDE's, together with linearity of the BC's controlling input of reactants and products to the pore. This result means that it suffices to determine $R^B_{tot}(f=0)$ for negligible conversion, since then $R^B_{tot}(f) = (1\text{-}f)\, R^B_{tot}(0)$. Then the reaction kinetics follow from $d/dt \langle A_{out} \rangle = -c\, R^B_{tot}(0) \langle A_{out} \rangle$ producing *exponential decay* of $\langle A_{out} \rangle$. The constant c equals the number of pores in the system divided by the total number of 3D lattice sites associated with the fluid and by X_{eq}.

Functionalization only of pore ends with catalytic sites

Next, we consider the case where only the 20 sites at each end of a pore of length L=100 are catalytic. Other parameters are selected as above. For $P_{ex}=0$, behavior is shown in Fig.3a. We find that a significant amount of A entering the pore "runs the gauntlet" to reach the non-reactive central region without conversion to B [13,14]. Thus, at the end of the first stage of pore filling, a significant blob of A remains in the pore center. Then, in a second much slower stage, this blob of A is converted to B via fluctuation-dominated diffusion from the center to the end reactive regions [14]. The pore center is devoid of A in the final steady-state. The profile is essentially the same as that when all sites reactive given that the penetration of reactant is well below 20 sites.

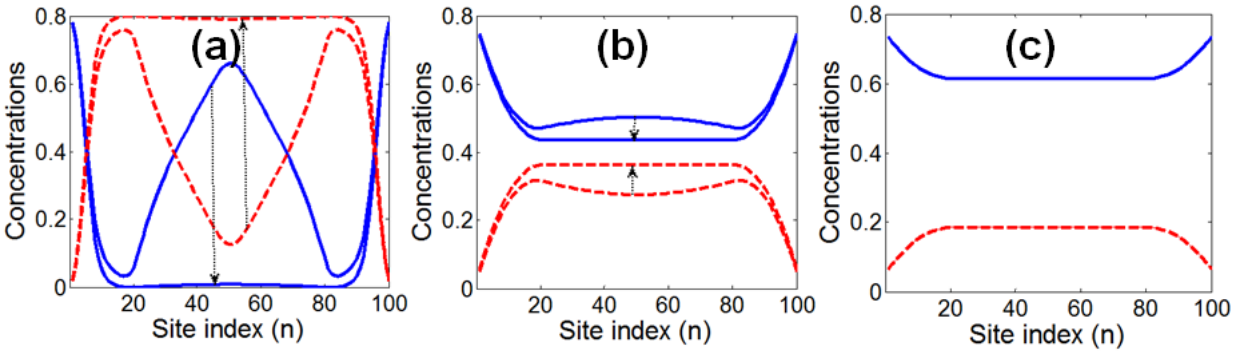

Figure 3. Steady-state concentration profiles for pores of length L=100 with just 20 catalytic sites on each end: **(a)** $P_{ex} = 0$ (single-file diffusion); **(b)** $P_{ex} = ¼$; and **(c)** $P_{ex} = 1$ (unhindered diffusion). Profiles are shown for a time corresponding to the peak A-concentration in the pore center, as well as for long time t = 60,000 [where the system reached the steady-state, or nearly so for (a)]. Arrows indicate time evolution (e.g., reducing the A concentration in the pore center). Other model parameters are: $W_{rx} = 0.001$, $W_{diff} = 1$, $\langle A_{out} \rangle = 0.8$, and $\langle B_{out} \rangle = 0$.

For P_{ex} = ¼ (Fig.3b), there is also a slight initial buildup of A in the pore center which diminishes for longer times. The final steady-state profile retains a significant uniform concentration of A in the center. This reflects the larger penetration of reactant (beyond 20 sites) for all sites reactive when P_{ex} = ¼. The uniformity of the steady-state concentration in unreactive regions follows from the governing equations. For P_{ex} = 1 (Fig.3c), the above trend is amplified, and now there is no transient maximum of concentration of reactant in the pore center.

CONCLUSIONS

The catalytic activity of mesoporous materials containing functionalized linear nanopores is shown to be strongly dependent of the propensity for passing of reactants and products within the pores. Limited passing means that most of completely functionalized pores are actually catalytically unproductive, being filled with "trapped" product. For this reason, pores with only the ends functionalized will have the same reactivity (unless passing of reactants and products is sufficiently facile that the reactant can penetrate to the central region of the pore).

ACKNOWLEDGMENTS

This work was supported by the Division of Chemical Sciences, Office of Basic Energy Sciences, U.S. Department of Energy (USDOE). It was performed at Ames Laboratory which is operated for the USDOE by Iowa State University under Contract No. DE-AC02-07CH11358.

REFERENCES

1. *Catalysis and Adsorption by Zeolites*; G. Ohlmann, H. Pfeifer, G. Fricke, Eds.; Elsevier, Amsterdam, 1991.
2. K. Tajima and T. Aida, *Nanostructured Catalysts*, Plenum, New York, 2003.
3. J.S. Beck, J.C. Vartulli, W.J. Roth, M.E. Leonowicz, C.T. Kresge, K.D. Schmitt, C.T.W. Chu, D.H. Olson, and E.W. Sheppard, J. Am. Chem. Soc. **114**, 10834-10843 (1992).
4. S. Huh, J.W. Wiench, J.-C. Woo, M. Pruski, and V.S.-Y. Lin, Chem. Mater. **15**, 4247 (2003).
5. C.-H. Tsai, H.-T. Chen, S.M. Althaus, K. Mao, T. Kobayashi, M. Pruski, and V.S.-Y. Lin, ACS Cat. **1**, 729 (2011).
6. T.E. Harris, J. Appl. Prob. **2**, 323 (1965).
7. J. Kärger and D. Freude, Chem. Eng. Technol. **25**, 769 (2002).
8. J.G. Tsikoyiannis and J.E. Wei, Chem. Eng. Sci, **46**, 233 (1991).
9. J. Kärger, M. Petzold, H.S. Pfieffer, S. Ernst, and J. Weitkamp, J. Catal. **136**, 283 (1992).
10. C. Rodenbeck, J. Kärger, and K. Hahn, Phys. Rev. E **55**, 5697 (1997).
11. M.S. Okino, R.Q. Snurr, H.H. Kung, J.E. Ochs, and M.L. Mavrovouniotis, J. Chem. Phys. **111**, 2210 (1999).
12. S.V. Nedea, A.P.J. Jansen, J.J Lukkien, and P.A.J. Hilbers, Phys. Rev. E **65**, 066701 (2002).
13. D.M. Ackerman, J. Wang, J.H. Wendel, D.-J. Liu, M. Pruski, and J.W. Evans, J. Chem. Phys. **134**, 114107 (2011).
14. D.-J. Liu, J. Wang, D.M. Ackerman, I.I. Slowing, M. Pruski, H.-T. Chen, V.S.-Y. Lin, and J.W. Evans, ACS Catalysis **1**, 751 (2011).
15. D.M. Ackerman, J. Wang, and J.W. Evans, Phys. Rev. Lett., submitted (2012).
16. R. Kutner, Phys. Lett. **81A**, 239 (1981).